



Discovery of high affinity ligands for β_2 -adrenergic receptor through pharmacophore-based high-throughput virtual screening and docking



Ruya Yakar^a, Ebru Demet Akten^{b,*}

^a Graduate School of Computational Biology and Bioinformatics, Kadir Has University, Cibali, 34083 Istanbul, Turkey

^b Department of Bioinformatics and Genetics, Faculty of Engineering and Natural Sciences, Kadir Has University, Cibali, 34083 Istanbul, Turkey

ARTICLE INFO

Article history:

Accepted 10 July 2014

Available online 21 July 2014

Keywords:

Virtual screening
Pharmacophore modeling
 β_2 -Adrenergic receptor
Docking
Scoring

ABSTRACT

Novel high affinity compounds for human β_2 -adrenergic receptor (β_2 -AR) were searched among the clean drug-like subset of ZINC database consisting of 9,928,465 molecules that satisfy the Lipinski's rule of five. The screening protocol consisted of a high-throughput pharmacophore screening followed by an extensive amount of docking and rescoring. The pharmacophore model was composed of key features shared by all five inactive states of β_2 -AR in complex with inverse agonists and antagonists. To test the discriminatory power of the pharmacophore model, a small-scale screening was initially performed on a database consisting of 117 compounds of which 53 antagonists were taken as active inhibitors and 64 agonists as inactive inhibitors. Accordingly, 7.3% of the ZINC database subset (729,413 compounds) satisfied the pharmacophore requirements, along with 44 antagonists and 17 agonists. Afterwards, all these hit compounds were docked to the inactive apo form of the receptor using various docking and scoring protocols. Following each docking experiment, the best pose was further evaluated based on the existence of key residues for antagonist binding in its vicinity. After final evaluations based on the human intestinal absorption (HIA) and the blood brain barrier (BBB) penetration properties, 62 hit compounds have been clustered based on their structural similarity and as a result four scaffolds were revealed. Two of these scaffolds were also observed in three high affinity compounds with experimentally known K_i values. Moreover, novel chemical compounds with distinct structures have been determined as potential β_2 -AR drug candidates.

© 2014 Elsevier Inc. All rights reserved.

1. Introduction

Human β_2 -ARs belong to the largest subfamily of G-protein-coupled receptors (GPCRs) in the human genome, which is the rhodopsin family. Also known as seven transmembrane domain receptors (7TM receptors), they are embedded in the cell membrane and have a crucial role in signal transduction from extracellular side to intracellular side in many different physiological pathways [1]. GPCRs deal with our physiological responses to hormones, neurotransmitters and environmental stimulants and they initiate many signaling pathways [2]. Thus, many diseases such as hypertension, depression, asthma, cardiac dysfunction, and inflammation, are related to the functioning of GPCRs [3], which is among the four gene families targeted by more than 50% of drugs on market [4–6].

In 2007, when Rasmussen and coworkers discovered the first X-ray crystal structure of the human β_2 -AR (PDB id: 2RH1) [7], a new gate was opened for computer-aided drug discovery. Novel β_2 -AR inhibitors have been introduced using structure-based and ligand-based computational algorithms [8–11]. Kolb et al. [9] screened a library of approximately 1 million compounds via docking using the X-ray structure (PDB id: 2RH1) and introduced twenty-five novel antagonists, which were tested in a radioligand binding assay. Six confirmed hits were identified with K_i values ranging between 9 nM and 3.2 μ M. Docking-based virtual screening experiments conducted by Topiol et al. [10,11] produced new chemical classes of hits besides rediscovering the well-known hydroxylamine chemotype. De Graaf and Rognan [12] modified the rotameric states of (Ser212) S5.43 and (Ser215) S5.46 within the binding site of the first X-ray structure, which represents the inactive state of β_2 -AR and created an “early activated” model, which was found to be more successful in distinguishing partial/full agonists from decoy ligands in docking runs. This study demonstrated the existence of small but critical differences between agonist- and antagonist-bound structures. Three X-ray crystal structures of β_2 -AR in complex with three antagonists revealed by Wacker et al. [13] also demonstrated minor

* Corresponding author at: Department of Bioinformatics and Genetics, Faculty of Engineering and Natural Sciences, Kadir Has University, Cibali, 34083 Istanbul, Turkey. Tel.: +90 212 533 65 32; fax: +90 212 533 43 27; mobile: +90 539 301 65 44.
E-mail address: demet.akten@khas.edu.tr (E.D. Akten).

local structural differences that exist in the binding pocket of these complexes. The docking-based virtual screening study performed by Vilar et al. [14] using the X-ray structure of β_2 -AR (PDB id: 2RH1) revealed that antagonists (blockers) were preferred over agonists. This was a promising result since the structure of the receptor used as a target was the apo form of the structure in complex with a partial inverse agonist carazolol and thus represents an inactive state. Moreover, using an ensemble of alternative conformations of the receptor generated to account for protein flexibility, they were able to increase the number of hits within the top 0.5% of the screened database.

Besides structure-based approaches, a ligand-based drug screening study by Tasler et al. [15] revealed a selective and potent human β_2 -AR antagonist. The screening was based on a pharmacophore alignment on known β_3 -adrenoceptor ligands, which generated a set of β -adrenoceptor ligands. Their binding affinities were measured in various binding assays. Upon further optimization of these ligands, a selective and potent human β_2 -AR antagonist with a K_i value of 0.3 nM was introduced.

In our current study, we present a virtual screening protocol that combines pharmacophore- and docking-based approaches to reveal high-affinity compounds for human β_2 -AR. The novelty of this work is the pharmacophore model, which has been generated using five different X-ray crystal structures of β_2 -AR in complex with five different antagonists. As of today, no virtual screening study based on structure-based pharmacophore modeling has been reported. The screened database was the “clean drug-like” subset of ZINC database [16]. A data set consisting of 64 known agonists and 53 known antagonists obtained from GLIDA database [17] was used to test the discriminatory power of the pharmacophore model. For the compounds that satisfied the pharmacophore requirements, a series of docking experiments have been conducted using the apo form of the inactive crystal structure (PDB id: 2RH1) as the target conformation. Compounds with highest binding affinities have been extracted and evaluated based on their predicted ADMET properties. Accordingly, a total of 62 molecules with high binding affinity and desirable ADMET properties have been extracted and were further classified based on their common functional groups.

2. Methods

2.1. Generation of the pharmacophore model

Five distinct inactive states of β_2 -AR were used to create a structure-based pharmacophore model using LigandScout software tool [18]. For each antagonist-bound complex structure extracted from Protein Data Bank (PDB ids: 2RH1, 3D4S, 3NY8, 3NY9, 3NYA), a pharmacophore model was generated. Then, a so-called “shared” pharmacophore model that solely consists of the features existing in all five models was constructed. Moreover, excluded volumes representing the sterically occupied regions by the receptor, were taken into account to increase the selectivity of the model.

2.2. Assessment of the pharmacophore model

To test the discriminatory power of the pharmacophore model, a database was created using 53 antagonists and 64 agonists obtained from GLIDA GPCR-Ligand Database [17]. Each molecule was selected based on its unique chemical composition to ensure its distinctiveness (See supplementary materials, Tables S1 and S2). The two antagonists, alprenolol and timolol, which were used to construct the pharmacophore model, also existed in this small database. LigandScout software tool was used to screen 53 antagonists as the active ligands and 64 agonists as the inactive ligands.

The maximum number of pharmacophore features that can be omitted during screening was set to 2. The hit compounds that satisfied the pharmacophoric requirements were evaluated with an in-house scoring function [18].

To evaluate the performance of the model to discriminate active ligands from inactive ones, the receiver operating characteristic (ROC) curve was constructed. Each point on the curve corresponds to the percentage of hit agonists versus the percentage of hit antagonists with a score value above a certain threshold. The so-called “model exhaustion” or the “cutoff” point where the slope of the ROC curve starts to become lower than 1 (slope of the diagonal line) was determined. The threshold value that corresponds to that “cutoff” point was then used for screening the ZINC database where the hit compounds with a score value below that threshold value were simply discarded. The remaining hit compounds were further evaluated through docking experiments.

2.3. ZINC database to be screened

The set of compounds to be screened was selected as the clean drug-like subset of ZINC database consisting of 9,928,465 molecules as of June 2012. This subset was especially selected because it lacked any aldehydes or thiols (also called “yuck” compounds). Also, all the compounds satisfied the Lipinski’s Rule of Five, with molecular weight less than 500 and higher than 150, octanol–water partition coefficient smaller than 5, number of hydrogen bond donors less than 5, number of hydrogen bond acceptors less than 10. In addition, the maximum number of rotatable bonds was set to 7 and polar surface area was less than 150 Å².

2.4. Evaluations through docking and scoring

The target protein was selected as the apo form of the inactive crystal structure after removal of the partial inverse agonist carazolol (PDB id: 2RH1). In the first docking stage, GOLD docking software tool with ChemPLP scoring function was used since it provided the shortest runtime with a relatively higher accuracy rate. Each run consisted of 10 runs confined in a spherical region of 10 Å radius in the binding pocket. The docked conformation with the highest ChemPLP score value, the so-called best pose, was selected and evaluated based on its neighboring residues interacting within a distance of less than or equal to 5 Å. There exist some well-known key residues for antagonist binding previously reported in experimental studies [13]; Ser203, Ser204 and Ser207 situated on one side of the binding pocket and Asp113, Val114 and Asn312 on the other side. Accordingly, the first criterion for satisfying the correct binding mode was to interact with at least one residue from each side of the binding pocket. The compounds that passed this critical binding test have been further evaluated based on their score value.

In the second stage of docking, the compounds with ChemPLP score values above a certain threshold were redocked to the same apo form of the receptor using AutoDock [19] and GOLD [20]. AutoDock performed 20 runs for each compound using Lamarckian genetic algorithm for conformational search and AutoDock’s semi-empirical scoring function. Dockings were confined in a grid box with dimensions of 22.5 Å × 22.5 Å × 22.5 Å and grid spacing of 0.375 Å. All 20 docked conformations from AutoDock were further evaluated with DSX scoring function [21] and the conformation with the highest DSX score value was selected. In parallel to AutoDock, GOLD performed 10 runs for each compound in a spherical region of 10 Å radius in the binding pocket using both GoldScore and ChemScore scoring functions, and likewise, the conformation with the highest score value was selected. Consequently, for each compound, a total of 3 docked conformations, each with the highest score value was determined from DSX, GoldScore and ChemScore, respectively.

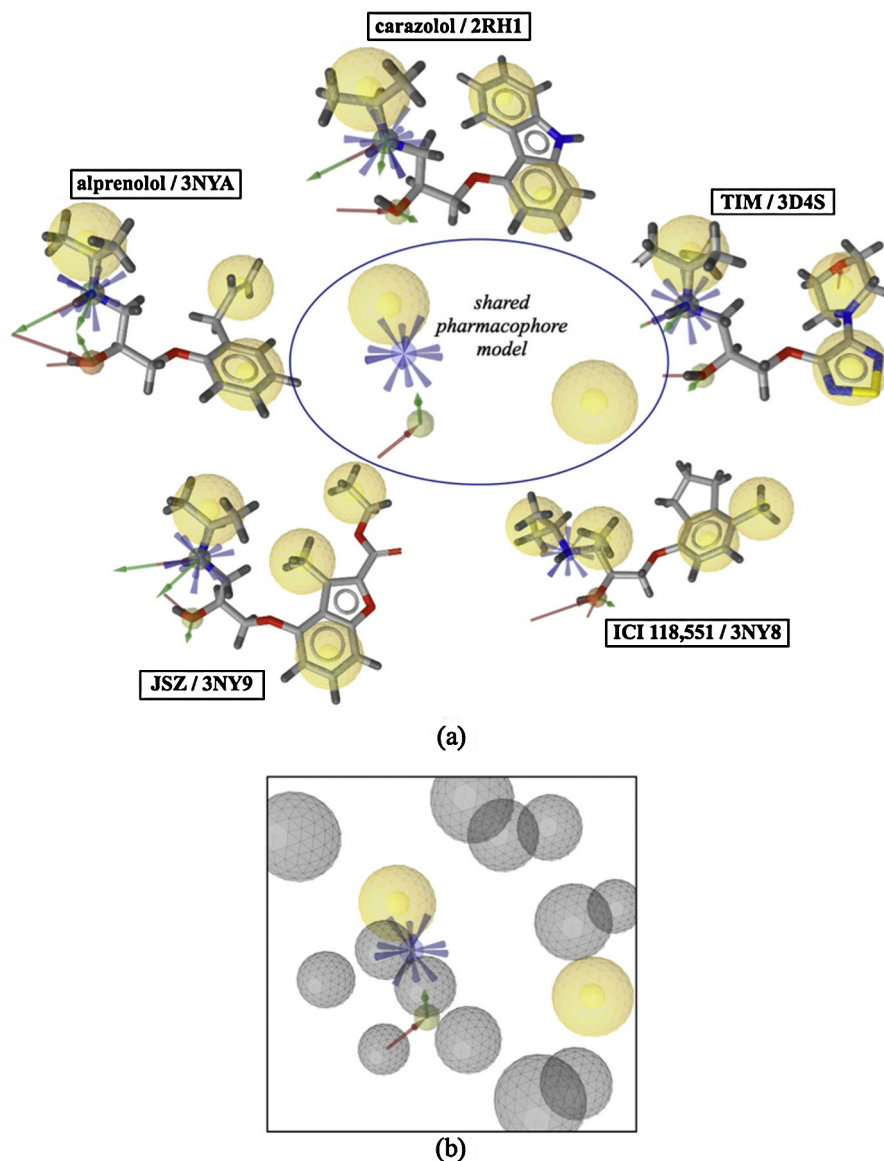


Fig. 1. Pharmacophore models of (a) five X-ray crystal structures of human β_2 AR illustrated with PDB ids and the bound antagonist/inverse agonist (b) the shared pharmacophore model with excluded volumes represented by gray spheres. Hydrophobic features are depicted with yellow spheres, hydrogen bond donor and acceptors by green and red arrows, and positive ionizable area by blue spheres. All models are illustrated by LigandScout software tool.

Each selected pose was further evaluated with a second binding test that was more stringent than the first one. Accordingly, the ligand has to interact with all four residues, Ser203, Asp113, Asn312, and Tyr316, and in addition, with either one of Tyr286 or Asn293 [13]. The compounds that fulfilled these binding criteria have been further evaluated according to their score values. Those with a score higher than a threshold value have been selected for the next stages of filtering. The threshold values were set to 150, 77 and 42 for DSX, GoldScore and ChemScore, respectively. Then, all selected compounds were merged into a single pool of hits; a compound was counted as a hit if it was selected in all three docking experiments.

Final evaluation of the hit compounds was performed using two ADMET descriptors provided by Discovery Studio tool of Accelrys [22]; human intestinal absorption (HIA) and blood brain barrier (BBB) penetration. The HIA property was determined using a pattern recognition model based on partition coefficient, $\log P$, and polar surface area, PSA and derived from a training set of 199 well-absorbed molecules with actively transported molecules removed. The BBB penetration of a molecule was defined as the ratio of

concentrations of the compound on both sides of the membrane after oral administration and predicted using a regression model based on 120 compounds with measured penetration. Both HIA and BBB models provide 95% and 99% confidence ellipses. In this study, the compounds that fell inside the 95% confidence ellipse for each HIA and BBB were proposed as plausible drug candidates.

3. Results

3.1. Stage I. Pharmacophore screening

The shared pharmacophore model was generated using the structural information of five inactive crystal structures in complex with five different inverse agonists and/or antagonists (PDB ids: 2RH1, 3D4S, 3NY8, 3NY9, 3NYA). As listed in Table S3, the pharmacophore model generated for each complex contains in average three or four hydrophobic features, also illustrated with yellow spheres in Fig. 1. Besides, each model holds in average three Hydrogen bond donors and two Hydrogen bond acceptor features, designated with green and red arrows, respectively. In all five

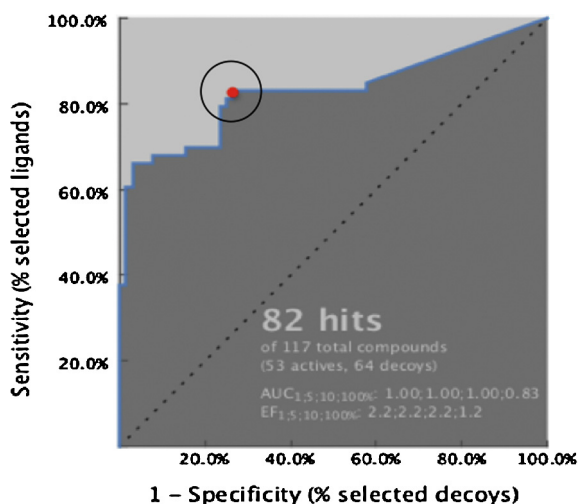


Fig. 2. Receiver Operating Characteristics (ROC) curve obtained from the screening of 117 molecules with known activities (53 agonists and 64 antagonists). $AUC_{1,5,10,100\%}$: 1.00; 1.00; 1.00; 0.83 and $EF_{1,5,10,100\%}$: 2.2; 2.2; 2.2; 1.2. The red dot illustrates the selected “model exhaustion” or the cut-off point.

ligands, there exists one single positive ionizable group located on the backbone Nitrogen atom and represented with a blue sphere. The so-called “shared” pharmacophore model that holds the features common to all five models consists of two hydrophobic features, one Hydrogen bond donor, one Hydrogen bond acceptor and one positive ionizable group, as depicted at the center of Fig. 1a. Additionally, to increase the selectivity of the model, a set of 13 excluded volume spheres that represents the sterically occupied region by the receptor was incorporated, as illustrated with gray spheres in Fig. 1b.

The small database composed of 53 antagonists as active ligands and 64 agonists as inactive ligands was screened using Ligand-Scout’s default parameters; scoring function taken as “Relative Pharmacophore Fit”, the number of omitted features set to 2, and check exclusion volume turned on. Fig. 2 illustrates the receiver operation characteristic (ROC) curve for 82 hit compounds satisfying the pharmacophore requirements out of 117 compounds in the dataset. The “model exhaustion” or “cut-off” point on the curve, corresponding to 27% false positives (17 out of 64 agonists) versus 83% true positives (44 out of 53 antagonists), was selected to represent all 61 molecules with a Relative Pharmacophore Fit value above 0.64. Consequently, the threshold value for the high-throughput screening of ZINC database was set to 0.64. A total of 729,413 hit molecules out of 9,928,495 molecules of the “Clean Drug-Like” subset of ZINC database passed the screening and were selected for further evaluation through various docking tools.

3.2. Stage II. Docking experiments: evaluations based on binding mode and score values

The first docking was performed using GOLD software tool conducted with ChemPLP scoring function since it provided fastest docking runs among other scoring functions. 729,413 molecules from ZINC database and 61 molecules from dataset were docked to the apo form of the inactive crystal structure (PDB id: 2RH1) within two months. For each compound, the conformation with the highest score was selected and evaluated based on the interacting residues as described in Materials and Method section (binding test #1). A total of 610,490 compounds from ZINC database and 58 molecules (41 antagonists and 17 agonists) have fulfilled the binding requirements of the first test. A threshold value of 85 was selected for ChemPLP score for further elimination. This value

corresponds to an enrichment factor of 11.9 for a 3.2% database coverage determined from, $ER = (TP/A)/(n/N)$. Here, TP is the number of true positives (known antagonists in our dataset), which is 17, whereas A is the total number of antagonists in the screened database, which is equal to 44. In the denominator, n is the number of selected hit compounds which is 23,588 and N is the total number of compounds in the screened database and is equal to 729,474. The number of selected hit compounds, 23,588, is simply the sum of 23,568 ZINC compounds, 17 antagonists and 3 agonists.

Furthermore, all 23,588 molecules were redocked to the same apo form of the receptor (PDB id: 2RH1) using AutoDock and GOLD software tools. 20 docked poses of AutoDock were rescored with DSX scoring function and the conformation with the highest DSX score was selected. Similarly, two scoring functions, GoldScore and ChemScore, were used to determine the conformation with the highest score among ten docked poses of GOLD. Each selected pose was further evaluated based on the interacting residues (the second binding test as described in Methods section). The number of compounds from ZINC database and the dataset satisfying the requirements of the second binding test is provided in the flowchart illustrated in Fig. 3. Accordingly, about 10,000 ZINC compounds’ best pose from each three docking experiments satisfied the second binding test. In addition, out of 17 antagonists, 11 to 13 antagonists were among the hit compounds.

It is also noteworthy that out of 17 agonists that passed the pharmacophore screening, only three agonists passed the ChemPLP filter and fulfilled the second binding requirements. Since they represent the false positives of the screening protocol, their binding mode as well as their interacting residues, were demonstrated in Fig. S1 in order to reveal some key features that can be used for further elimination. Clearly, all three agonists are large molecules with at least three cyclic groups and resemble to the antagonists and the hit compounds. Moreover, all three interact with the key residues and were oriented in a similar direction in the binding site (see carazolol as reference in Fig S1 for comparison). Thus, their ability to pass the initial stages of the screening test were not surprising considering their molecular size and their orientation in the binding pocket. Additional docking experiments with various scoring functions became inevitable to eliminate them from the hit list.

For further elimination, the threshold values for DSX, GoldScore and ChemScore have been set to 150, 77, and 42, respectively. The compounds with score values below these thresholds have been discarded. Then, all the remaining molecules were merged into the same pool; they were counted as a hit if they satisfied all three thresholds. Consequently, 360 compounds from ZINC database and three antagonists from dataset were selected as hits and further evaluated based on ADMET (Absorption, Distribution, Metabolism, Extraction and Toxicity) properties, using Discovery Studio tool by Accelrys [22]. It is noteworthy that no agonist was found among the hit list since the three threshold values (150, 77, and 42) have been selected such that no agonist would be left after the merge. Furthermore, approximately two thirds of the hit compounds were eliminated after each docking evaluation by DSX, GoldScore and ChemScore, and when the results were merged, only a few hundred compounds were left for analysis in more detail and within a reasonable time frame.

3.3. Stage III. Human intestinal adsorption and blood brain barrier predictions

The human intestinal absorption (HIA) and the blood brain barrier (BBB) penetration were estimated by ADMET module of Discovery Studio tool. From dataset, only one antagonist molecule, Carvedilol, was detected inside two confidence ellipses provided for HIA and BBB predictions (see Fig. S2a). On the other hand, among 360 compounds from ZINC database, 62 molecules

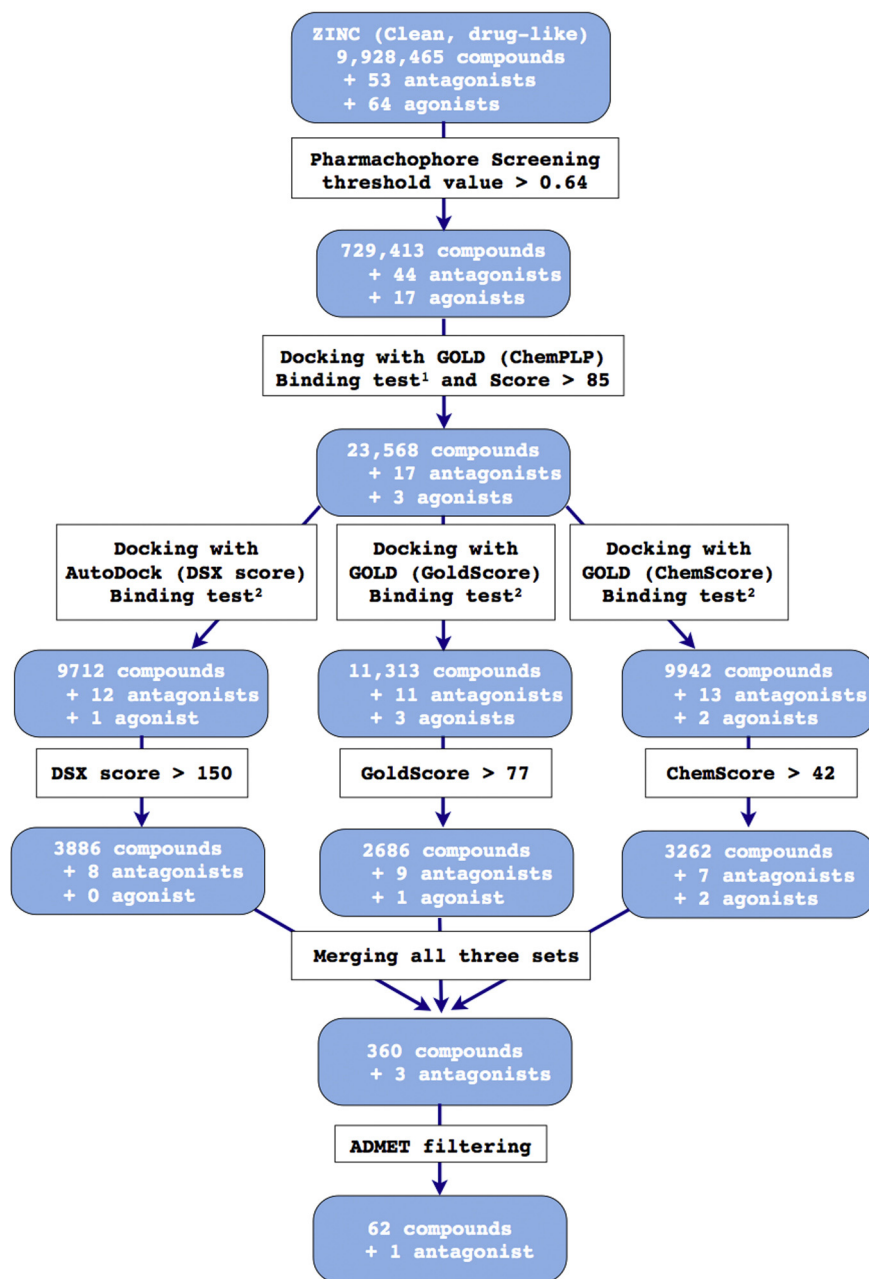


Fig. 3. Flowchart of the screening process of the Clean Drug-Like ZINC database and the dataset.

were found inside two 95% and 99% confidence ellipses as illustrated in Fig. S2b. For further analysis, these 62 molecules were selected and were further classified based on their chemical structure.

4. Discussion

4.1. A closer look at the drug candidates for novel scaffolds

Fig. 4 illustrates 62 molecules' best poses from AutoDock after being rescored with DSX, ChemScore and GoldScore to validate that they bind properly in the binding pocket surrounded by key interacting residues. The partial inverse agonist Carazolol in the inactive crystal structure (PDB id: 2RH1) was illustrated as a reference state in all four snapshots. Clearly, the best pose of each

62 compound, especially those generated by AutoDock runs (see Fig. 4b), share a unique orientation that matches well with that of Carazolol, besides interacting with the same key residues inside the binding pocket. This clearly indicates the uniqueness of the binding orientation, which arises from making the required set of interactions.

To identify the chemical groups on the ligand that interact with the target receptor, the 2D chemical structure of all 62 molecules has been carefully investigated. Their 2D representations alongside their ZINC ID and compound names were provided in Table S4, as a supplementary material. Different isomeric forms of a molecule might possess very distinct binding modes, which might lead to different binding affinities. Therefore, the isomeric forms of some of the proposed candidates should not be discarded and considered in the future binding assays as well. 7 of those molecules were found to be the isomer of another compound in the same set. Thus, the

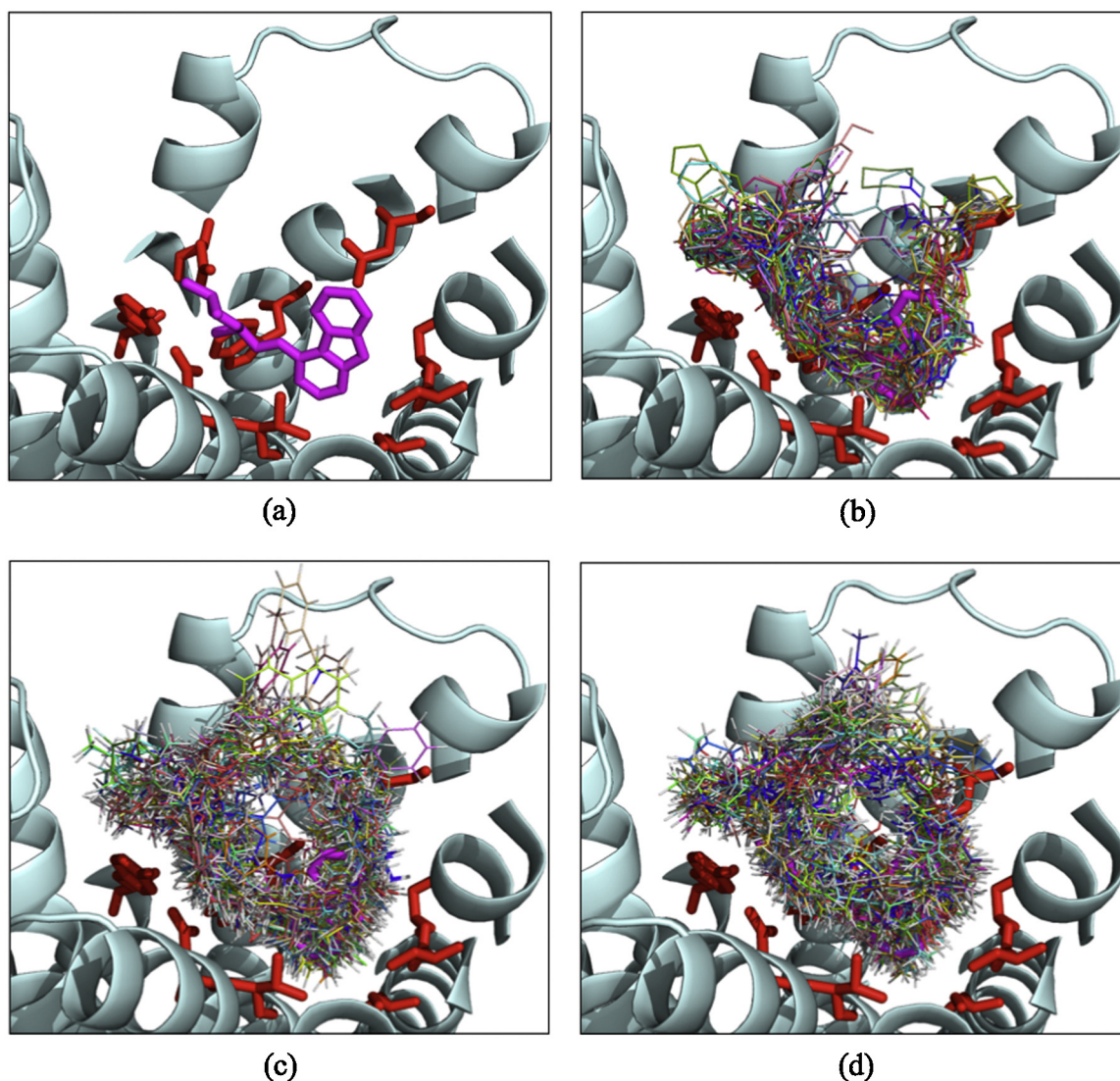


Fig. 4. (a) Partial inverse agonist Carazolol found in the X-ray crystal structure (PDB id: 2RH1) demonstrated in magenta color and stick representation for reference. Docked poses of 62 molecules with the highest score obtained from (b) AutoDock-DSX, (c) GOLD/GoldScore and (d) GOLD/ChemScore docking runs. Key residues for antagonist binding represented in red color and stick representation.

remaining 55 molecules were further classified according to their fixed part or the so-called “scaffold”. Four different scaffolds have been determined as listed in Table 1. The number of compounds that holds the scaffold #1, #2, #3, and #4 was found to be 25, 10, 6, and 8, respectively. Additionally, one single compound holds the carazolol scaffold and the remaining 5 molecules had unique structures as illustrated in Fig. 5. For each scaffold in Table 1, the 2D structure of an example hit compound that holds the corresponding scaffold was illustrated as well. The well-known classical scaffold of β_2 AR ligands composed of a β -hydroxy-amine motif and an ether group, as listed in Table 1, holds a partial resemblance with scaffold #3 and #4; the amine group in the classical scaffold is replaced by a six-membered ring in scaffold #3 and #4, that is the piperazine with two amine groups and the morpholine group with an amine and ether functional groups, respectively. Moreover, the widely known alprenolol scaffold also illustrated in Table 1 was found in three hit compounds that include the scaffold #4.

Besides their structural similarities, there exist significant overlaps between the binding modes of scaffold #3, #4 and carazolol. Fig. 6a illustrates all 6 compounds that hold the scaffold #3 with key interacting residues and the carazolol. The six-membered ring in all

six compounds coincides well with the corresponding amine group of carazolol, making similar interactions with Asn312 illustrated in 2D interaction plots (supplementary figures, Figs. S3, S4). The oxygen atom of carboxamide side group in Asn312 makes a hydrogen bond with backbone amine group in carazolol (Fig. S3), whereas it makes hydrogen bond with the nitrogen atom in the heterocyclic ring of one of the hit compounds (Fig. S4). At the opposite side, all the hydroxy and the ether groups of the hit compounds are well aligned with those of carazolol as shown in Fig. 6a. Consequently, the oxygen atom of hydroxyl group in both carazolol and the hit compound makes a second hydrogen bond with the nitrogen atom of carboxamide side group in Asn312 (Figs. S3, S4).

The main difference between carazolol and the hit compounds with scaffold #3 is in the hydrophobic tail facing the transmembrane helix 5 (TM5). In carazolol, Ser203 makes a hydrogen bond with the amine group of the carbazole tail that is not present in the hydrophobic heterocyclic ring of any of the hit compounds. Moreover, the propanyl end group of carazolol coincides with the large aromatic group in all six compounds (denoted as R_1 in Fig. 6a), which expands towards the entrance of the binding cavity, interacting with Lys305 on TM7, Asp192 on ECL2, His93 on TM2, Trp109 on

Table 1
List of scaffolds determined for 62 hit compounds along with the well-known alprenolol and carazolol scaffolds.

Scaffold type	Scaffold 2D	Example hit compound
1		
2		
3		
4		
Alprenolol		
Carazolol		

TM3. On the other hand, the hydrophobic catecholamine group in carazolol coincides well with the aromatic moiety denoted as R_2 in all six compounds, making hydrophobic interactions with Tyr199, Ser207, Val114 and Phe290.

Fig. 6b illustrates all 8 compounds with scaffold #4. The only difference between scaffold #3 and #4 is the six-membered ring that has an ether and an amine functional groups in scaffold #4, whereas it has two amine groups in scaffold #3. Similarly, the heterocyclic ring coincides well with backbone amine group in carazolol, as

well as the hydroxy and the ether groups that line up with those of carazolol. The 2D interaction plot for one of the hit compound (Fig. S5) shows the hydroxy group making three hydrogen bonds with Asp113, Asn312 and Tyr316, whereas the hydroxy group in carazolol interacts only with Asn312.

Similar to hit compounds with scaffold #3, there exist a large aromatic tail that coincide with the short propanyl end group of carazolol. This aromatic tail is represented by R_1 group in Fig. 6b, which expands towards the entrance of the binding cavity,

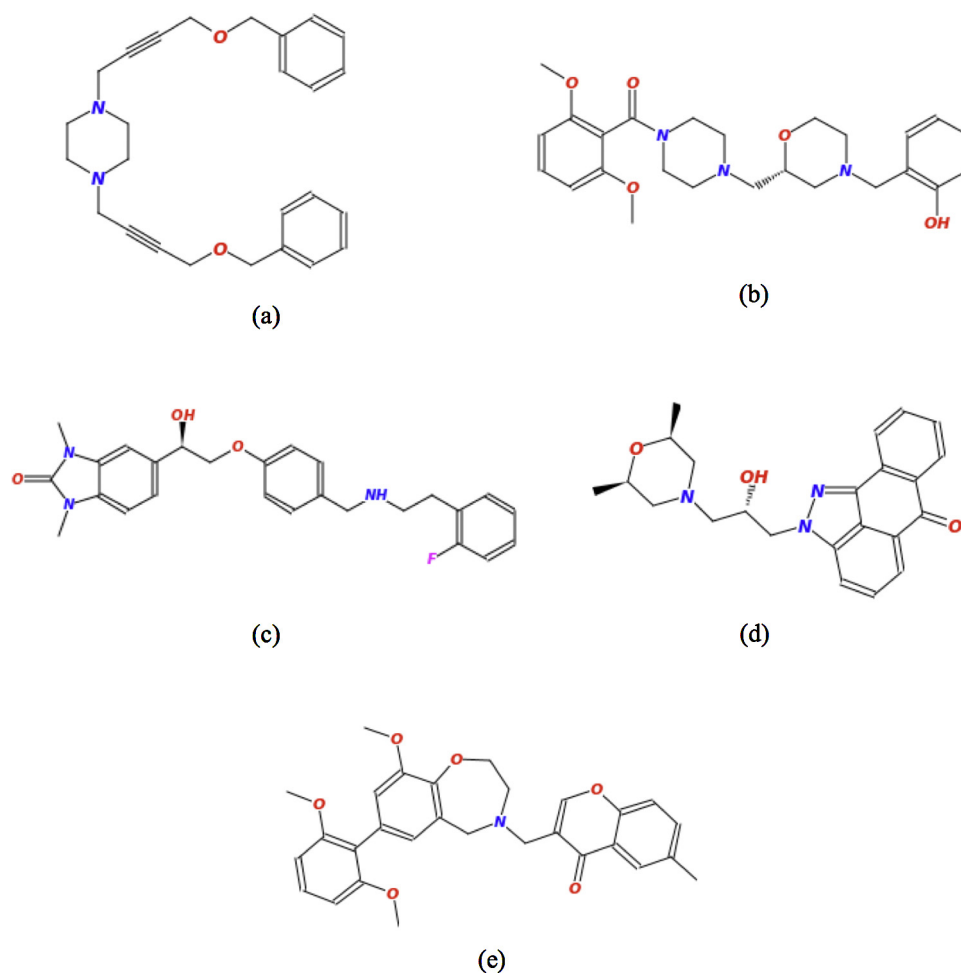


Fig. 5. 2D representation of the five compounds with unique structures. (a) ZINC19367103; 1,4-di(4-benzyloxy-2-butynyl)piperazine hydrochloride, (b) ZINC34691828; (2,6-dimethoxyphenyl)-[4-[[[(2S)-4-[(2-hydroxyphenyl) methyl]morpholin-2-yl]methyl]piperazin-1-yl]meth], (c) ZINC40721209; 5-[(1R)-2-[4-[[2-(2-fluorophenyl)ethylamino]methyl]phenoxy]-1-hydroxy-ethyl]-1,3-dimethyl-benzimidazole, (d) ZINC66482925; [(2S)-3-[(2S,6R)-2,6-dimethylmorpholin-4-yl]-2-hydroxypropyl]BLAHone and (e) ZINC67674643; 3-[[7-(2,6-dimethoxyphenyl)-9-methoxy-2,3-dihydro-1,4-benzoxazepin-4(5H)-yl]methyl]-6-methyl-4H-chromen-4-one.

interacting with Tyr308 and Ile309 on TM7, His93 and Ile94 on TM2, Cys191 and Asp192 on ECL2, and Trp109 on TM3. Moreover, the hydrophobic catecholamine group in carazolol lines up well with the single 5-membered or 6-membered cyclic ring denoted as R_2 in the hit compounds, making hydrophobic interactions with Ser203, Ser207, Val114 and Phe290 (see Fig. S5).

Structural alignments of the hit compounds for scaffold #1 and #2 with carazolol were illustrated in supplementary material Fig. S6. The glycineamide group in scaffold #1 coincides well with the backbone amine, hydroxy and ether groups of carazolol. In addition, most of the hit compounds were found to be correctly oriented along the well-known native state of carazolol. The scaffold #2 has the smallest functional group among others, which is simply a methanamide group. A total of 10 hit compounds with scaffold #2 aligned to carazolol show a satisfactory orientation in the binding pocket, making necessary interactions with key residues.

The best pose of the five hit compounds that do not incorporate any of the scaffolds listed in Table 1 are illustrated with carazolol in Fig. 7. The first compound, which is the only hit with a carazolol scaffold, has a satisfactory orientation with its backbone amine, hydroxy and ether groups all coinciding well with those of carazolol. The second compound is the antagonist carvedilol, which is a nonselective beta-blocker (beta1, beta2), and alpha-blocker

(alpha1) and was the only compound from dataset that passed all the filtering tests. It is found to be oriented suitably in the binding pocket with a conformation nearly matching that of carazolol. The aromatic methoxyphenoxy ring in carvedilol is lined up towards the entrance of the binding pocket, similar to hit compounds that hold scaffold #3 and #4.

4.2. Binding modes of the five hit compounds with unique structures

The best pose of the five hit compounds that do not hold any of the scaffolds mentioned so far are observed to be correctly oriented alongside carazolol, as illustrated in Fig. 7c–g. Four of these compounds are longer than carazolol with their extra aromatic tails extending to the entrance of the binding pocket between TM2 and TM7, where it interacts with Gly90, His93, and Ile94 on TM2, Ile309 and Trp313 on TM7, and, Cys191 and Phe193 on ECL2. Consequently, the binding cavity becomes more tightly packed with the ligand, which leaves a small amount of space for other small molecules. Another common feature of these five compounds is that they all contain at least three aromatic groups. Moreover, three of these groups contain an amine group that always aligns well with the backbone amine group of carazolol.

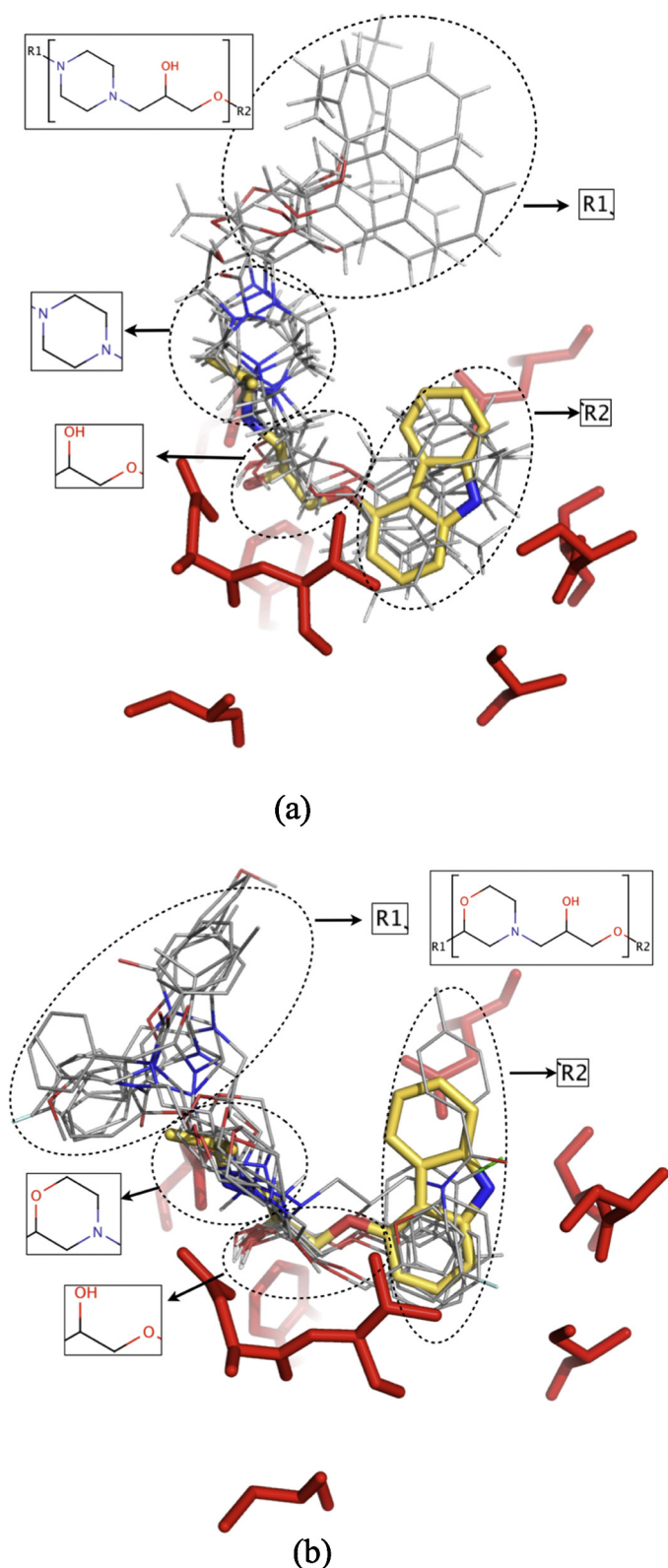


Fig. 6. Hit compounds that hold (a) the scaffold #3 and (b) the scaffold #4 with key interacting residues shown with red sticks and the carazolol in yellow. (For interpretation of the references to colour in this figure legend, the reader is referred to the web version of this article.)

The compound #1 has a symmetric structure with a piperazine group in the center and two 4-benzyloxy-2 butynyl groups on each side (see Fig. 5). The nitrogen on the piperazine group coincides well with the backbone amine group of carazolol (see Fig. 7c). Although the ligand lacks any hydrogen bond with the receptor, it interacts with a total of 21 residues, including all the essential ones (see supplementary material Fig. S7). This is a significant amount of interactions compared to carazolol surrounded by 14 residues only (Fig. S3). Its symmetric structure is another novel feature for being a candidate for a beta-blocker.

The second compound has a *piperazine* group attached to a morpholine group at the center, and a 2,6-dimethoxyphenyl and a 2-hydroxyphenyl group on each side as illustrated in Fig. 5. It makes three hydrogen bonds with Tyr316, Asn312 and Asn293, surrounded by a total of 19 residues (see supplementary material Fig. S8). It fits in a favorable orientation in the binding pocket, lining up well with carazolol (see Fig. 7d). The nitrogen atom on the piperazine group plays the role of the backbone amine group in carazolol, making hydrogen bond with Asn312 as in carazolol. Besides, the aromatic tail hydroxyphenyl group expands towards the entrance of the binding pocket between TM2 and TM7 as the benzyl group in compound #1.

The third compound has a benzodiazole-2-one and a fluoro-phenyl group on each side (see Fig. 5). Similar to compound #2, it is well aligned with carazolol (see Fig. 7e), interacts with 19 residues and makes three hydrogen bonds with Ser203, Asp113 and Asn312 and has an aromatic tail that expands towards the entrance (Fig. S9). The oxygen atom on the hydroxyl group makes two hydrogen bonds with both Asp113 and Asn312 simultaneously. The third hydrogen bond is between the oxygen atom in the side group of Ser203 and the oxygen atom on benzodiazole of the ligand, which coincides in position with the nitrogen of the aromatic ring in carazolol.

The fourth compound has a large aromatic moiety similar to that in carazolol (see Fig. 5). The oxygen atom on the aromatic group makes a hydrogen bond with Ser203 that similarly interacts with the nitrogen atom of the aromatic group in carazolol (see Figs. S3 and S10). Moreover, two more hydrogen bonds are observed between the ligand and Asn312, in a strikingly similar way as in carazolol. Unlike the other four compounds, it has a short aromatic tail represented by the morpholine group attached to two methyl groups, that matches well with the propanyl amine tail of carazolol. Overall, it aligns suitably with carazolol as illustrated in Fig. 7f.

Finally, the fifth compound is composed of three aromatic groups; a dimethoxyphenyl, a benzoxazepin and a methylchromene-4-one group (see Fig. 5). It sits nicely inside the binding pocket and is lined up with carazolol. The nitrogen atom on the benzoxazepin group coincides in space with the backbone amine group in carazolol (see Fig. 7g). It interacts with 16 residues among which Phe193 on ECL2, Thr110 on TM3 and His93 on TM2 are making hydrogen bonds with the hydroxyl groups located on two aromatic groups of the ligand that expands upward (see Fig. S11).

4.3. Similarities to compounds with known activities

Fig. 8a shows the 2D representation of a new compound proposed by Tasler et al. [15] that shows a strong binding affinity to human β_2 AR with an experimentally measured K_i value of 1.2 nM. The compound has an alprenolol scaffold, with R_1 group as isopropyl, and R_2 group as the morpholine that was commonly encountered in the hit compounds. Consequently, it holds the scaffold #4 listed in Table 1. Another work by Sabio et al. [11] proposed two novel compounds that also show strong binding affinities with experimentally measured K_i values of 0.311 ± 0.09 nM and

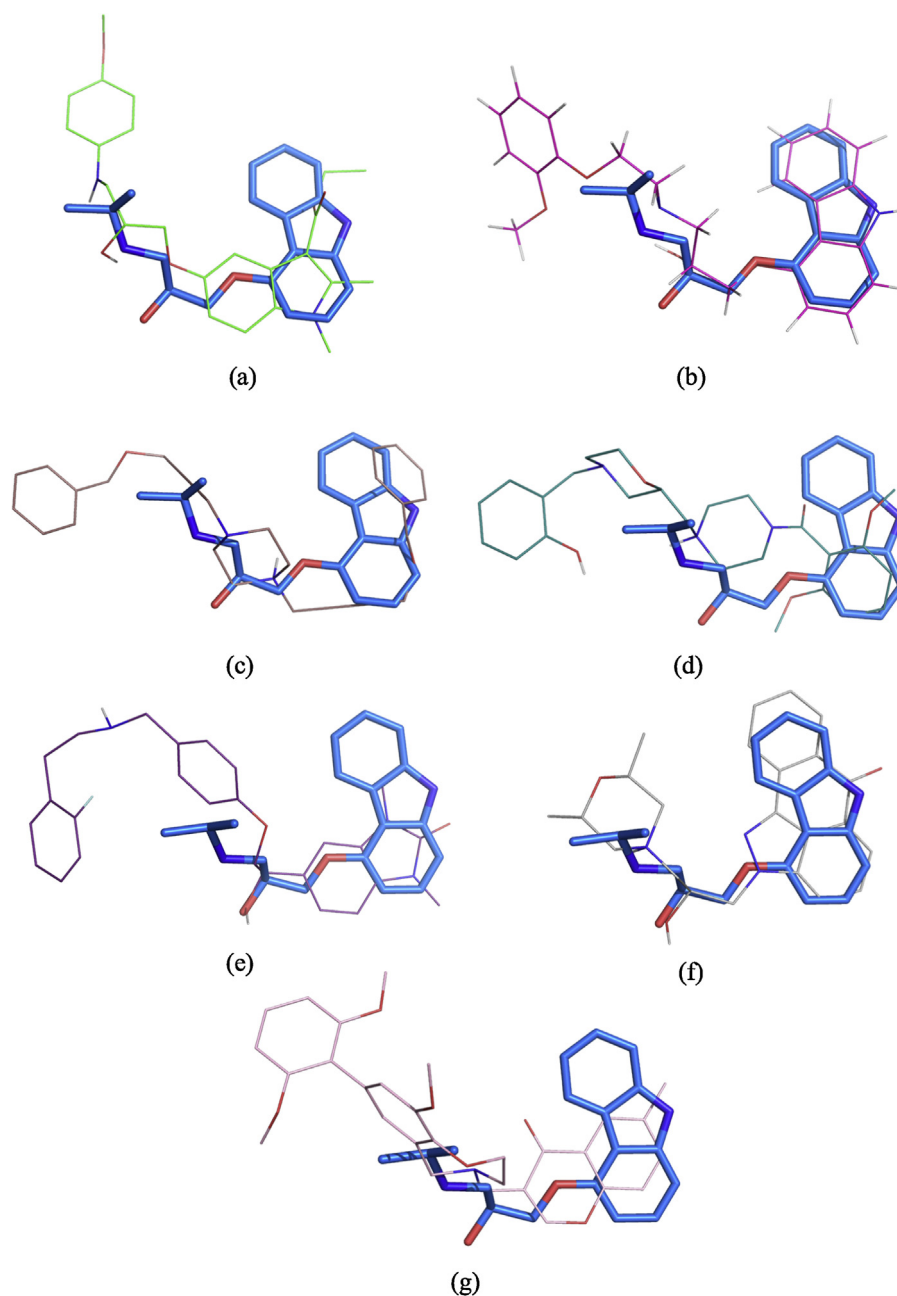


Fig. 7. Best poses of (a) the hit compound with carazolol scaffold, (b) carvedilol and (c)–(g) the five hit compounds with unique structures. Carazolol represented by stick model in blue as a reference. (For interpretation of the references to colour in this figure legend, the reader is referred to the web version of this article.)

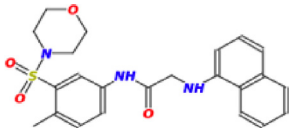
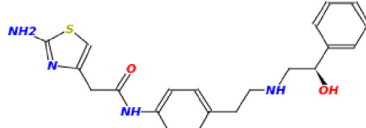
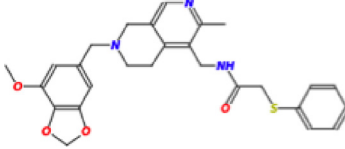
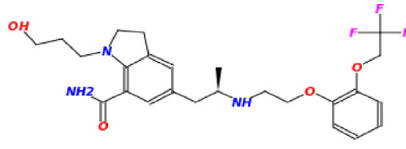
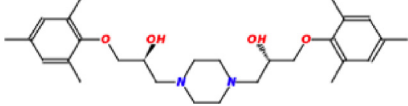
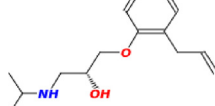
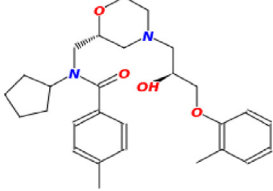
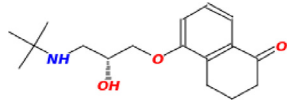
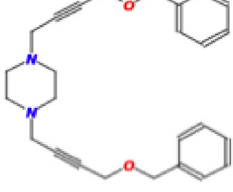
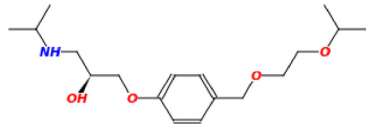
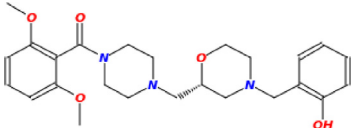
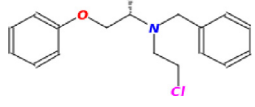
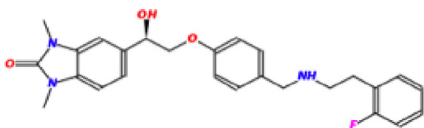
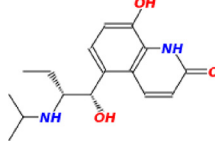
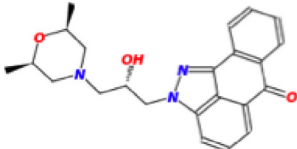
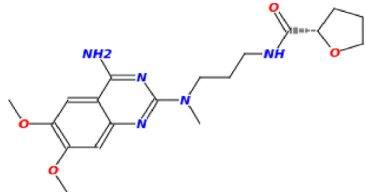
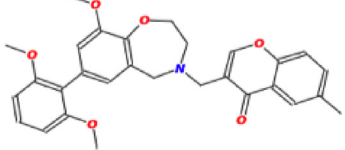
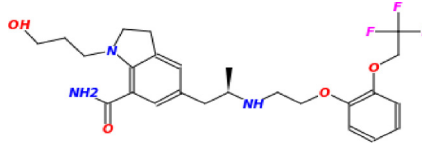
57.3 ± 1.6 nM. Remarkably, both compounds hold the scaffold #3 with piperazine group and diphenylmethane as R_1 group, as illustrated in Fig. 8b and c. The R_2 group has an indole in both compounds, one attached to a methyl and the other to a carbonitrile.

Timolol and landiolol are two important beta-blockers and both contain morpholine groups [25,26]. Furthermore, the activity of 2 DPM derivatives (2-(3,4-dihydroxyphenyl)morpholines 3 and 4) with a morpholinic structure has been reported by Maccia et al. [27] in radioligand binding assays and functional tests on isolated preparations and exhibited similar adrenergic receptor activity with norepinephrine and isoprenaline. Also, piperazine group is found in antianginal drugs, Ranolazine and Trimetazidine for the treatment of chronic

angina pectoris. Beta-blockers are also classified as antianginal medications.

Finally, a representative compound from each scaffold and the five unique compounds have been searched as query in Drug-Bank database which contains nearly 7000 drug entries to identify approved drug molecules that share some similarities with our proposed hit compounds. The first four entries in Table 2 belong to the representative compounds from each scaffold, which broadly resemble known antagonists with the highest Tanimoto coefficient ranging between 0.395 and 0.735. On the other hand, the five compounds with unique structures have the corresponding Tanimoto coefficient between 0.369 and 0.483. Especially, the two hit compounds (IDs **1** and **8**) with T_c values below 0.4 present novel scaffolds not previously explored.

Table 2
List of hit compounds, their nearest antagonists in DrugBank [23], their identity and their corresponding Tanimoto similarity.

ID	Structure	Nearest antagonists in Drug Bank	Identity	T _c
1			Mirabegron a beta3 adrenergic receptor agonist	0.395
2			Silodosin an alpha1-adrenoceptor antagonist	0.433
3			Alprenolol an adrenergic beta-antagonist	0.735
4			Levobunolol a nonselective beta-adrenoceptor antagonist	0.554
5			Bisoprolol a cardioselective beta1-adrenergic antagonist	0.407
6			Phenoxybenzamine an alpha-adrenergic antagonist	0.452
7			Procaterol a long-acting beta2-adrenergic receptor agonist	0.483
8			Alfuzosin an alpha-adrenergic blocker	0.369
9			Silodosin an alpha1-adrenoceptor antagonist	0.418

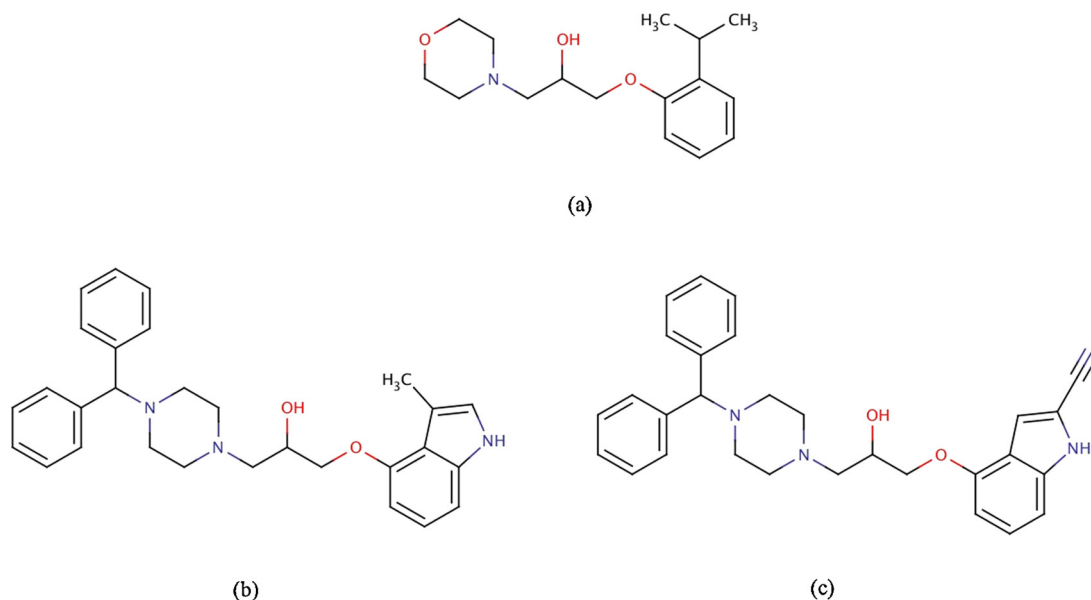


Fig. 8. 2D representation of (a) compound #35 proposed by Tasler et al. [15], (b) compound #3 and (c) compound #11 proposed by Sabio et al. [11].

5. Conclusions

A shared pharmacophore model generated from five known inactive crystal structures of human β_2 AR was used to screen the clean-drug like subset of ZINC database consisting of 9,928,465 compounds for the discovery of novel β_2 AR antagonists. Pharmacophore-based screening yielded 729,413 compounds that were docked to the apo form of one of the five inactive crystal structures. Following a series of docking/rescoring, a total of 360 compounds were found to satisfy the requirements for key residues and score values, and were sent to ADMET filtering. 62 compounds have fulfilled the requirements for human intestinal absorption (HIA) and blood brain barrier penetration and thus were proposed as potential binders. These compounds were further analyzed and classified based on their common functional groups. Four distinct scaffolds have been detected. Remarkably, a novel compound proposed by Tasler et al. [15], possess one of our proposed scaffolds with a morpholine group. This compound was experimentally shown to have a strong binding affinity to human β_2 AR with a K_i value of 1.2 nM. Moreover, timolol and landiolol, two important beta-blockers both contain morpholine groups.[25,26] In addition, Sabio et al. [11] proposed two novel compounds from their screening studies for which the experimental binding affinities were measured as 0.311 ± 0.09 nM and 57.3 ± 1.6 nM. Likewise, both compounds were found to hold one of the four proposed scaffolds with the piperazine group. At the end, screening millions of compounds through several stages of filtering, yielded 62 hit compounds with noticeable structural similarities to those with strong binding affinities tested experimentally. In addition, novel scaffolds have been discovered with low similarities to any known approved drugs. Although the experimental validation of these compounds are lacking, computational methods predicts them as strong binders. Furthermore, the pharmacophore model, which was based on the structure of receptor–antagonist complex, increases the probability of these compounds to function as antagonists than as agonists.

Conflict of interests

The authors declare that they have no competing interests.

Acknowledgments

This work has been partially supported by The Scientific and Technological Research Council of Turkey (TÜBİTAK, Project # 109M281) and Kadir Has University BAP (Project # 2010-BAP-04).

Appendix A. Supplementary data

Supplementary material related to this article can be found, in the online version, at <http://dx.doi.org/10.1016/j.jmgm.2014.07.007>.

References

- [1] P.A. Marjin, S. Verhoeven, C. de Graaf, L. Roumen, B. Vrolijk, B.S. Nabuurs, J. de Vlieg, P.G. Klomp, *J. Chem. Inf. Model.* 51 (2011) 2277–2292.
- [2] D.M. Rosenbaum, S.G. Rasmussen, B.K. Kobilka, *Nature* 459 (2009) 356–363.
- [3] M.O. Becker, Y. Marantz, S. Shacham, B. Inbal, A. Helfetz, O. Kalid, S. Bar-Halm, D. Warshaviak, M. Fichman, S. Noiman, *Proc. Natl. Acad. Sci. U.S.A.* 101 (2004) 11304–11309.
- [4] K. Lundstrom, *Curr. Protein Pept. Sci.* 7 (2006) 465–470.
- [5] J.P. Overington, B. Al-Lazikani, A.L. Hopkins, *Nat. Rev. Drug. Discov.* 5 (2006) 993–996.
- [6] S. Schlyer, R. Horuk, *Drug Discov. Today* 11 (2006) 481–493.
- [7] S.G.F. Rasmussen, H.J. Choi, M.D. Rosenbaum, T.S. Kobilka, S.F. Thian, C.P. Edwards, M. Burghammer, R.P.V. Ratnala, R. Sanishvili, F.R. Fischetti, F.X.G. Schertler, I.W. Weis, B.K. Kobilka, *Nature* 450 (2007) 383–388.
- [8] M. Wada, E. Kanamori, H. Nakamura, Y. Fukunishi, *J. Chem. Inf. Model.* 51 (2011) 2398–2407.
- [9] P. Kolb, D.M. Rosenbaum, J.J. Irwin, J.J. Fung, B.K. Kobilka, B.K. Shoichet, *Proc. Natl. Acad. Sci. U.S.A.* 106 (2009) 6843–6848.
- [10] S. Topiol, M. Sabio, *Bioorg. Med. Chem. Lett.* 18 (2008) 1598–1602.
- [11] M. Sabio, K. Jones, S. Topiol, *Bioorg. Med. Chem. Lett.* 18 (2008) 5391–5395.
- [12] C. de Graaf, D. Rognan, *J. Med. Chem.* 51 (2008) 4978–4985.
- [13] D. Wacker, G. Fenalti, M.A. Brown, V. Katritch, R. Abagyan, V. Cherezov, R.C. Stevens, *J. Am. Chem. Soc.* 132 (2010) 11443–11445.
- [14] S. Vilar, G. Ferinoia, S.S. Phatak, B. Berka, C.N. Cavasotto, S. Costanza, *J. Mol. Graph. Model.* 29 (2011) 614–623.
- [15] S. Tasler, R. Baumgartner, A. Aschenbrenner, A. Ammendola, K. Wolf, T. Wieber, J. Schachtner, M. Blisse, U. Quotschalla, P. Ney, *Bioorg. Med. Chem. Lett.* 20 (2010) 3399–3404.
- [16] J.J. Irwin, K.B. Shoichet, *J. Chem. Inf. Model.* 45 (2005) 177–182.
- [17] Y. Okuno, J. Yang, K. Taneishi, H. Yabuuchi, G. Tsujimoto, *Nucleic Acids Res.* 34 (2006) 673–677.
- [18] G. Wolber, T. Langer, *J. Chem. Inf. Model.* 45 (2005) 160–169.
- [19] G.M. Morris, R. Huey, W. Lindstrom, M.F. Sanner, R.K. Belew, D.S. Goodsell, A.J. Olson, *J. Comput. Chem.* 30 (2009) 2785–2791.
- [20] G. Jones, P. Willett, R.C. Glen, *J. Mol. Biol.* 245 (1995) 43–53.

- [21] H. Gohlke, M. Hendlich, G. Klebe, *J. Mol. Biol.* 295 (2000) 337–356.
- [22] W.J. Egan, K.M. Merz, J.J. Baldwin, *J. Med. Chem.* 43 (2000) 3867–3877.
- [23] D.S. Wishart, C. Knox, A.C. Guo, S. Shrivastava, M. Hassanali, P. Stothard, Z. Chang, J. Woolsey, *Nucleic Acids Res.* 34 (Database issue) (2006) D668–D672.
- [24] R.A. Laskowski, M.B. Swindells, *J. Chem. Inf. Model.* 51 (2011) 2778–2786.
- [25] J. Ogata, T. Okamoto, K. Minami, *Can. J. Anaesth.* 50 (2003) 753.
- [26] T.J. Zimmerman, H.E. Kaufman, *Arch. Ophthalmol.* 95 (1977) 601–604.
- [27] B. Macchia, A. Balsamo, M.C. Breschi, A. Lapucci, A. Lucacchini, F. Macchia, C. Manera, A. Martinelli, C. Martini, E. Martinotti, S. Nencetti, *J. Med. Chem.* 35 (1992) 1009–1018.